Advanced Ceramics Progress: Vol. 10, No. 1, (Winter 2024) 22-33

Materials and Energy Research Center
MERC

Contents lists available at ACERP

Advanced Ceramics Progress

Journal Homepage: www.acerp.ir

Original Research Article

Physical, Mechanical, and Microstructural Characteristics of Al-MMCs Incorporating Zirconium Diboride Particles Fabricated by Warm Equal Channel Angular Pressing Method

Hossein Jafari [a], Masoud Rajabi [b,*], Mehdi Montazeri-Pour [c]

[a] *PhD Candidate, Department of Materials Science & Engineering, Faculty of Technology and Engineering, Imam Khomeini International University (IKIU), Qazvin, Iran.*
[b] *Associate Professor, Department of Materials Science & Engineering, Faculty of Technology and Engineering, Imam Khomeini International University (IKIU), Qazvin, Iran.*
[c] *Assistant Professor, Department of Chemical and Materials Engineering, Buein Zahra Technical University (BZTE), Buein Zahra, Qazvin, Iran.*

* Corresponding Author Email: m.rajabi@eng.ikiu.ac.ir; masoudrajabi@yahoo.com (M. Rajabi) URL: https://www.acerp.ir/article_208071.html

ARTICLE INFO

Article History:
Received: 23 December 2023
Revised: 15 March 2024
Accepted: 07 September 2024

Keywords:
Al Metal Matrix Composites,
Mechanical Milling,
Equal Channel Angular Pressing,
Physical Properties,
Zirconium Diboride Ceramic Particles,
Microstructural Analysis

ABSTRACT

This study evaluated the influence of mechanical milling time on the physical, mechanical, and microstructural properties of Al metal matrix composites (MMCs) incorporating ZrB_2 ceramic reinforcement. The mixing powders of aluminum with zirconium diboride were mechanically milled at different times. Then, the achieved composite powder was heated, compacted, and turned into bulk material by equal channel angular pressing (ECAP) at 250°C. SEM micrographs indicated that the size of the obtained particles decreases by increasing the mechanical alloying time by up to 18 hours. However, the particle size has increased after this time. The average size of fine particles reached 823nm using mechanical alloying for 18 hours, while coarse particles were 8µm. The size calculation of crystallites using XRD examination implied that the rate of crystallite size reduction after 12 hours of mechanical alloying is gradually reduced and reached its lowest level after 18 hours. Then, increasing the mechanical alloying time led to an increase in the size of the crystallites and a decrease in the lattice strain. The microstructure of resultant bulk composites has been characterized by optical microscopy (OM) and SEM. The bulk composite samples processed by the ECAP method, with an optimum amount of ZrB_2 (5 wt.%), had a relative density, hardness, shear yield stress, and ultimate shear strength of 99.3%, 170 HV, 125 MPa and 151 MPa, respectively, utilizing powders which were mechanically milled for 24 hours.

https://doi.org/10.30501/acp.2024.431922.1143

1. INTRODUCTION

The preparation of materials with excellent strength and flexibility has always been the interest of various researchers worldwide. Metal matrix composites (MMCs) are materials composed of one or more metallic elements as matrix and reinforcement. The synthesis of MMC powder is performed in different ways. Mechanical alloying is one of the production methods of MMC powder, which occurs through the reaction between the surfaces of reactive materials. Other

Please cite this article as: Jafari, H., Rajabi, M. & Montazeri-Pour, M. (2024). Physical, Mechanical, and Microstructural Characteristics of Al-MMCs Incorporating Zirconium Diboride Particles Fabricated by Warm Equal Channel Angular Pressing Method, *Advanced Ceramics Progress*, 10(1), 22-33. https://doi.org/10.30501/acp.2024.431922.1143

conventional methods cannot produce powders of metal composites, intermetallic compounds, etc., fabricated by this technique (Chak et al., 2020; Sharma et al., 2024). In recent years, aluminum-based composites have generally attracted the attention of several researchers owing to their low weight and high corrosion resistance to the harsh environment (Bhoi et al., 2019; Gajević et al., 2022). The use of these composites in the automotive industry, aerospace industry, and metal structures is progressive (Bhat et al., 2021; Chandel et al., 2021; Gajević et al., 2022). Strength is the most essential factor in the selection of these composites (Lakshmikanthan et al., 2022). The production of aluminum composites using the mechanical alloying method has been widely investigated (Erturun et al., 2021; Hamilton et al., 2021). The reinforcement of aluminum-based composite with secondary phase particles such as oxides, carbides, borides, and nitrides makes a suitable combination of physical and mechanical properties of both phases of the composites. Furthermore, the amount, size, and distribution of secondary phase particles determine the main properties of the composite (Diler and Ipek, 2012). ZrB_2, as a reinforcing phase with a very high melting temperature of 3250°C, high strength and hardness, chemical stability, and suitable electrical conductivity, has been the focus of many researchers in fabricating metal matrix composites. Pure ZrB_2 is brittle, and its combination with a soft metal could improve its mechanical and corrosion properties (Kumar and Kumar, 2022). Combining this ceramic material with ductile materials could result in composites with high strength and toughness (Kumar et al., 2021).

The severe plastic deformation (SPD) techniques cause changes in its mechanical and microstructural properties by applying a very high strain to the metal matrix composite (Brodova et al., 2021; Montazeri-Pour et al., 2014). The initial and final cross-section areas generally do not vary during straining in these processes (Montazeri-Pour et al., 2015a). Different methods of severe plastic deformation have been carried out. A few of its common types are equal channel angular pressing (ECAP) (Vishnu et al., 2020), high-pressure torsion (HPT) (Edalati and Horita, 2016), and accumulative roll bonding (ARB) (Ebrahimi and Wang, 2022), etc. (Faraji et al., 2018; Montazeri-Pour et al., 2015b). The ECAP process, as shown in Figure 1, is one of the most common methods of extreme plastic deformation, in which the sample is passed through an angular die, and the strain applied to the sample creates an ultrafine grain (UFG) microstructure. Improving mechanical properties results from creating a UFG microstructure using this intense plastic deformation (Montazeri-Pour et al., 2014).

The aim of this study is to evaluate the properties of the aluminum−zirconium diboride metal matrix composites with UFG structure obtained by the mechanical alloying process, where different times of milling have been considered to determine the optimal time required to attain the desired mechanical and physical properties as well as the formation of a UFG structure. Then, the bulk samples were obtained using the warm ECAP method, and their mechanical properties and microstructure were examined by performing mechanical tests, optical microscopy and SEM observations.

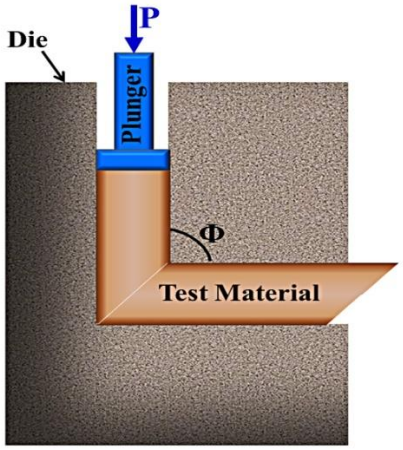

Figure 1. A schematic of the pressing method in ECAP die

2. MATERIALS AND METHODS

2.1. Initial Materials

The starting materials applied in this study were aluminum powders (99 wt.% purity and mean particle size (D) <20µm) and ZrB_2 (99 wt.% and D <5µm), which were purchased from the Chinese company of Jiaozuo Huasu Chemical Co.

SEM micrographs related to pure Al powder and primary ZrB_2 powder are given in Figure 2.

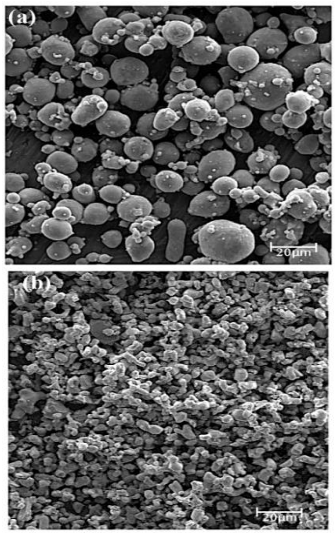

Figure 2. SEM images for (a) pure aluminum powder and (b) pure zirconium diboride powder

2.2. Production of Composite Powders

Pure aluminum powder and a mixture of 5 wt.% ZrB_2 plus pure aluminum powders were milled at room temperature under an argon atmosphere for 1, 6, 12, 18,

and 24 hours using a planetary ball mill with a capacity of 200ml and a rotation speed of 360rpm. The container was made of hardened steel, and the balls used in this process were made of stainless steel.

The total powder weight for this process was 20g, and the weight ratio of balls to powder was 1:15. Stearic acid (2 wt.%) was used as a process control agent (PCA) to prevent excessive cold welding of powder particles. The numbers, weights, and sizes of the balls are given in Table 1.

TABLE 1. Specifications of the balls used in the mechanical alloying process for the synthesis of Al-ZrB_2 MMC powder

Diameter (mm)	Weight (g)	The number of balls
5	0.65	30
8	2.09	20
10	4.02	15
13	8.96	13
20	32.52	2

2.3. Compaction of Composite Powders

Bulk samples were produced using the warm ECAP method in a die with an angle of Φ=90º. For this purpose, the desired powder was first placed in a copper sheath, as illustrated in Figure 3. The powder sheath in the copper tube was performed to reduce the friction of the sample with the mold and prevent the powder's dispersion during compaction. The average applied pressure was 20 tons/cm^2, the punch movement rate was 1.5 mm/s, and the working temperature was 250°C. The mold's inlet and outlet channels diameter was 12.70mm, and the lubricant used was MoS_2 powder.

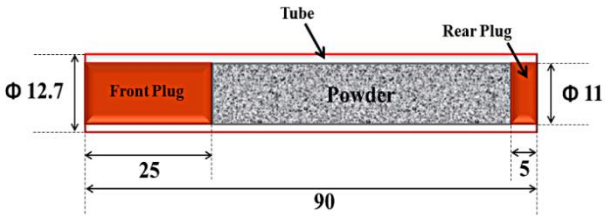

Figure 3. The copper sheath used in the compaction of powder by the warm ECAP method

2.4. Characterization of Produced Samples

Scanning electron microscopy (SEM) and optical microscopy (with a polarized camera) were used to examine the microstructure. An X-ray diffraction (XRD) test is utilized to identify the phase. Williamson-Hall Equation was used according to the following formula to evaluate the size of crystallites and lattice strain:

$$\beta\cos\theta = \frac{k\lambda}{D} + 4\varepsilon \sin\theta \qquad (1)$$

where θ indicates the diffraction angle of the peak, β denotes the width of the peak at half of the maximum height, and λ presents the X-ray wavelength.

The Archimedes equation was used according to the Equation 2 to measure the density of the samples (ASTM B311-22, 2022):

$$\rho = \frac{W_{air}\left[\rho_{water} - 0.0012\right]}{0.99983\left[W_{air} - W_{water}\right]} + 0.0012 \qquad (2)$$

where W_{air} and W_{water} represent the weight of the sample in air and in distilled water, respectively. The density ratio (ρ_{air}/ρ_{water}) is set to 0.0012 (Gao et al., 2021).

The samples used for the shear punch test were cut from a longitudinal section with a dimension ratio of H/D=1.5 (Figure 4 (a)), and then they were polished with soft sandpaper. The shear punch test device used was Datek, and the surface of the device jaw was lubricated to prevent friction between the jaw and the sample.

First, the samples were cut transversely from the middle part to perform the Vickers micro-hardness (HV) test on the samples (Figure 4 (b)), and the hardness was taken from different points using a Bohler micro-hardness tester with a load of 25, 120, 200, and 400gf. Finally, sandpaper 600 was used to prepare the surface of the samples to check the hardness more closely.

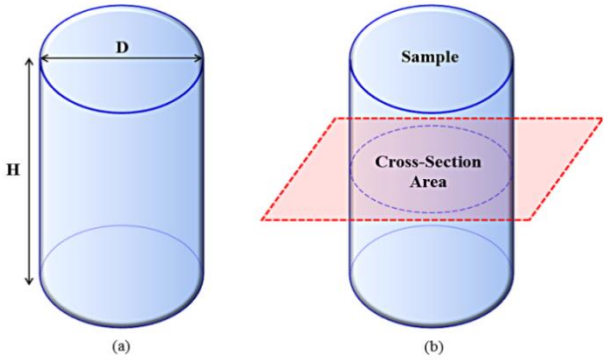

Figure 4. Cut samples prepared for use in (a) shear punch test and (b) Vickers micro-hardness (HV) test

3. RESULTS AND DISCUSSION

3.1. Powders Characteristics

3.1.1. X-Ray Pattern of Powders

XRD experiment was performed on samples at various times. The XRD of pure Al and Al-ZrB_2 powders mechanically milled from 1 hour to 24 hours is given in Figures 5 and 6, respectively.

As shown in Figure 5, the peaks related to (100), (200), (220), and (311) aluminum planes appeared at the diffraction angles of 38.463°, 44.723°, 65.073°, and 78.183°, respectively. In Figure 6, the (0001) plane appeared at an angle of 36.573° for the resulting Al-5wt.% ZrB_2 MMC powder in addition to the mentioned planes.

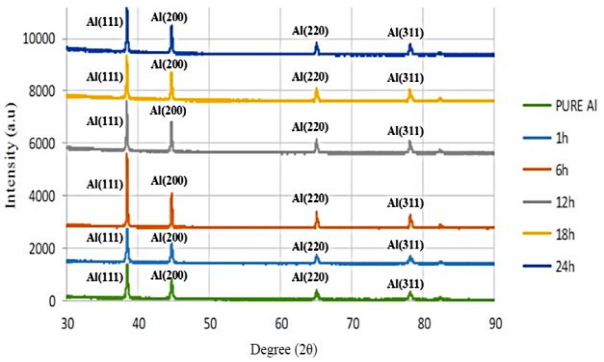

Figure 5. XRD of pure Al powder samples milled for 1, 6, 12, 18 and 24 hours

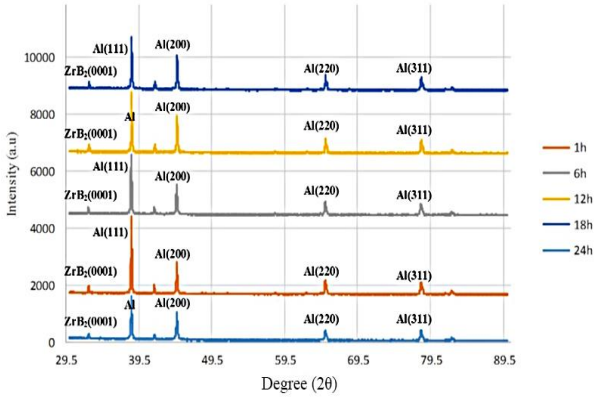

Figure 6. XRD of composite powder samples of Al-ZrB_2 (5wt.%) milled for 1, 6, 12, 18 and 24 hours

The possible reason for the peak appearance of the active (0001) plane of the hexagonal ZrB_2 structure is due to the lower energy of these planes compared to the aluminum FCC structure. In addition, the emergence of this peak is also likely due to the high percentage of ZrB_2 with a hexagonal structure (5% by weight). The peak of the reinforcing material is not observable in lower amounts (less than 1% by weight) due to the smaller size of the particles and their low dispersion compared to the matrix powder (Yue et al., 2017). A noteworthy point in the X-ray diffraction analysis of the samples is the absence of the aluminum oxide (Al_2O_3) peak in the graph, which is consistent with previous studies (Zhang et al., 2016).

Crystallite size and lattice strain were measured, and an analysis was performed on the samples using the Williamson-Hall formula, Equation (1). According to Figure 6, increasing the milling time leads to eliminating or reducing the intensity of additional peaks. Figure 7 shows the change in the position of the peaks relative to those of the initial samples during one up to 24h mechanical alloying. According to Figure 7, the peak angle has changed and is inclined to the left with the increase in the milling time due to the rise in the dissolution of the secondary phase. The diffusion of ZrB_2 into the aluminum lattice and its dissolution could be the reason for this issue. This phenomenon is consistent with the findings of other researchers (Patra et al., 2016; Suryanarayana, 1999). As shown, the intensity of the peak increased after 6 hours, and then the intensity of the peak decreased, but its width increased.

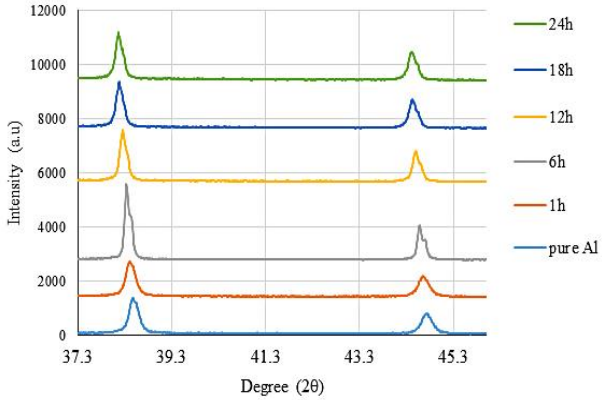

Figure 7. The changes in the position of peaks by increasing milling time for a mixture of pure Al and 5wt.% ZrB_2 powder

The graph of crystallite size and lattice strain of the powder samples is illustrated in Figure 8. The size of the crystallites decreased with the increase of milling time, and the lattice strain (calculated by the Williamson-Hall relation) increased. The equilibrium point of the curve means the time as the increase rate of the lattice parameter is declined, which specifies the equilibrium time of the two samples. This increased rate may be considered when finding the optimal time.

The change in the shape of powder particles during milling increases crystal defects such as point defects and dislocations. Defects increase the lattice strain and its internal energy and instability. The dislocations arrange themselves into a lower energy state, leading to low-angle boundaries forming. In longer milling times, the misalignment angle between the sub-grains increases due to more plastic deformation and more dislocations, and their boundaries become high-angle boundaries. Thus, the sub-grains become sub-micron grains. In addition, the size of crystallites for Al-ZrB_2 MMC powder is smaller than that of Al powder for each milling time, which could be due to the high hardness of ZrB_2 particles, reducing crystallite size during milling and facilitating the formation of nano-crystalline particles. In general, the decrease in the size of the crystallites with the increase in the milling time may be attributed to the generation and propagation of dislocations due to severe plastic deformation.

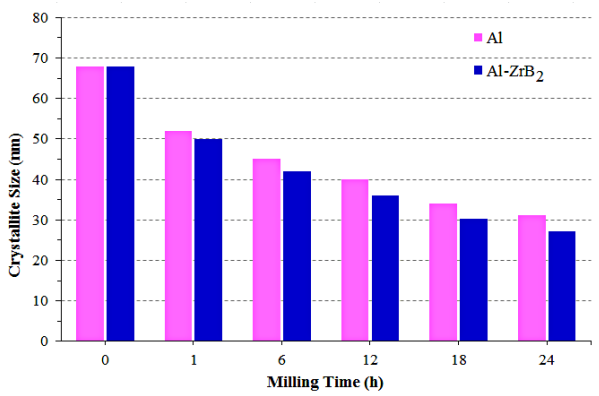

(a)

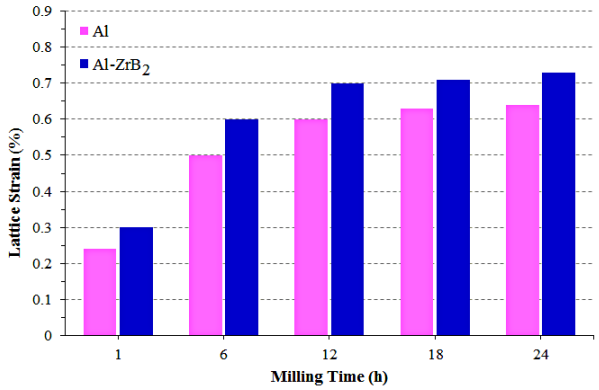

(b)

Figure 8. Changes in (a) size of crystallites and (b) lattice strain for Al and Al-5wt.% ZrB_2 MMC powders in terms of milling time at 1, 6, 12, 18 and 24 hours

In addition, the lattice strains increased up to 24 hours for both powders. This issue may be caused by dislocations, impurities, and other lattice defects during milling. Milling for more than 18 hours does not significantly affect the strain level. In addition, the lattice strain for each milling time is higher for the metal matrix composite than pure Al due to the presence of ZrB_2. The diffusion of ZrB_2 in the Al lattice and its interaction with dislocations may have increased the density of dislocations and then enhanced the strain in the particles.

3.1.2. The Microstructure of Powders

SEM images related to pure aluminum and Al-5wt.% ZrB_2 MMC powders resulting from the mechanical alloying process are shown in Figures 9 and 10, respectively.

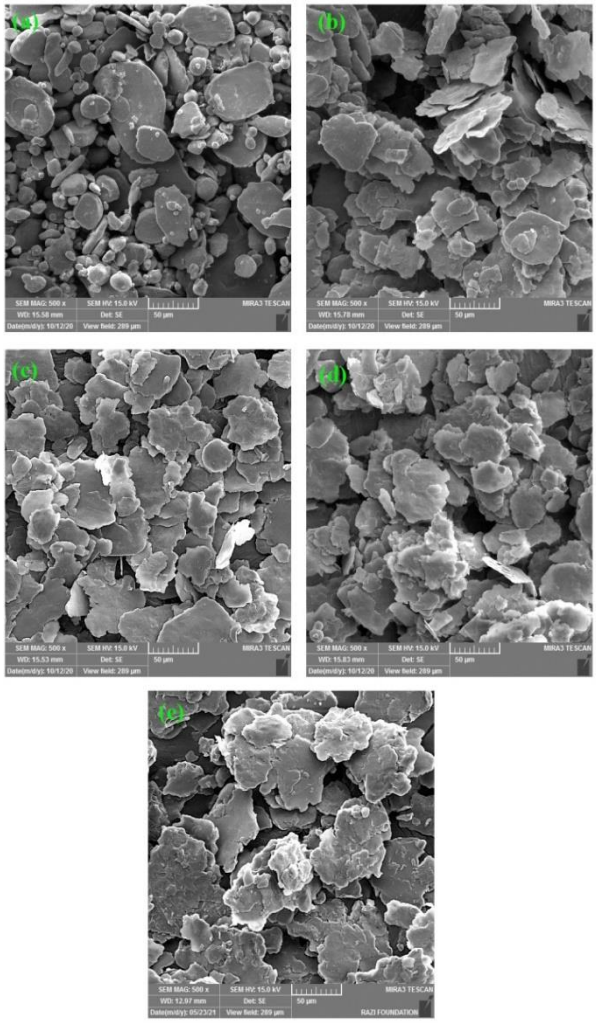

Figure 9. SEM images for samples of pure aluminum powder obtained from milling for (a) 1 hour, (b) 6 hours, (c) 12 hours, (d) 18 hours, and (e) 24 hours

The particle size decreased with increasing milling time. However, a more homogeneous structure was obtained by increasing the time to 12 hours. The dominant phenomena in the process of mechanical alloying are cold welding between particles and their fractures. In the early stages of milling (up to 6 hours), cold welding is the dominant phenomenon due to the softness of the particles. As a result, particle size is expected to increase, and the average particle size at this stage is 16µm. The phenomenon of fracturing the particles leads to their refinement after this stage, and along with the hardening of the particles, this phenomenon reaches its maximum value at 18 hours (Figure 10 (c) and (d)), which could be due to the balance of the two mentioned phenomena. Meanwhile, fine particles have taken up most of the powder volume, but some coarse particles are still visible in the structure. The average size of the refined grains at this stage has reached 823nm, and the coarse grains have reached 8µm. The 18

hours of mechanical alloying could be the optimum time to obtain a homogeneous microstructure. The determining mechanisms were in balance at this stage; however, after this stage, an average increase in the size of the particles was seen (Figure 10 (e)).

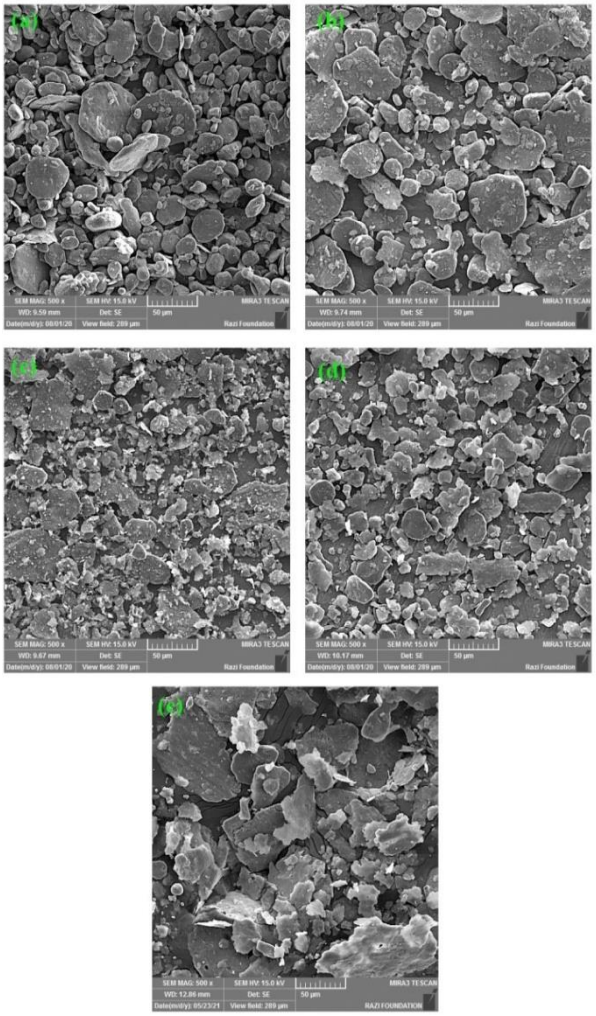

Figure 10. SEM images of Al-ZrB_2 MMC powders obtained from mechanical alloying of pure Al and 5wt.% ZrB_2 mixture powders for (a) 1 hour, (b) 6 hours, (c) 12 hours, (d) 18 hours and (e) 24 hours

The formation of spangle-shaped particles (Figure 11) after 12 hours of pure aluminum powder milling is observed by SEM in the microstructure of the samples. The reason for this could be the asymmetric accumulation of hardened particles and the cold welding of aluminum particles.

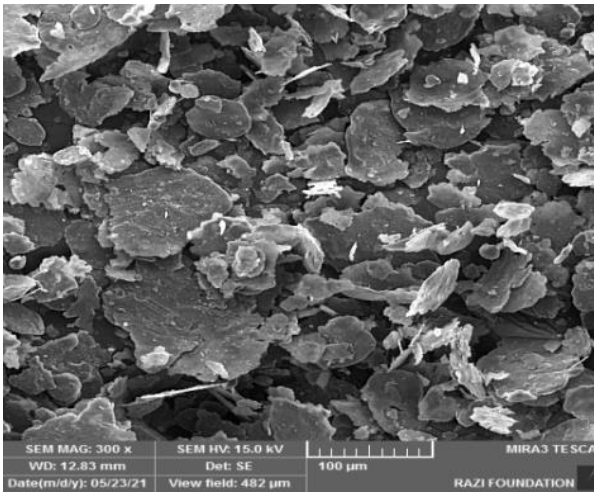

Figure 11. SEM images of milled aluminum powder representing the formation of spangle-shaped particles after 12 hours of milling

3.1.3. The Effect of Milling Time on Particle Size

Figure 12 demonstrates the size of Al particles and Al-ZrB_2 MMC powder obtained from mechanical alloying in terms of time. Increasing the time of mechanical alloying up to 12 hours has led to a significant reduction in the size of the particles. However, no significant reduction in the size of the particles has been achieved after this time. Increasing the mechanical alloying to more than 18 hours led to an increase in the particle size, indicating that 18 hours is the time to reach a stable state. The cold welding and particle fracture reach equilibrium (Maurice and Courtney, 1994). As shown, the slope of the variations between different milling times is higher for Al-ZrB_2, indicating that the addition of 5% ZrB_2 by weight has a significant effect on reducing the particle size by milling.

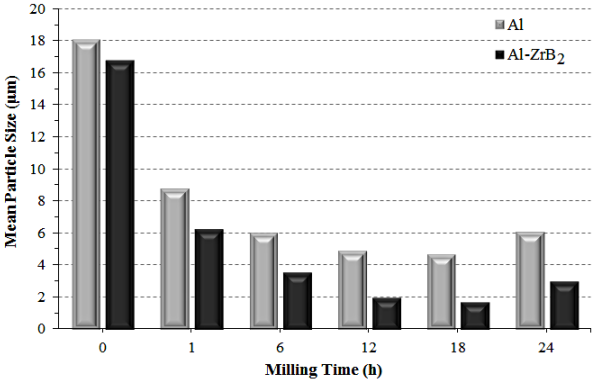

Figure 12. The effect of milling time on the particle size of pure Al and Al-ZrB_2 powders

3.2. Characteristics of Samples Subjected to ECAP

3.2.1. Physical Features of Bulk Samples

The warm ECAP method was used at 250°C to manufacture bulk pure aluminum and composite samples

from powders obtained by the mechanical alloying process. The consolidation of the 1-hour milled powders could not be performed, and the sample was incapable of bulking. The relative density and porosity percentage of the resulting bulk samples are given in Figure 13. As the milling time increased further, the porosity percentage of the resulting samples decreased. Activating dynamic recovery by increasing the milling time eliminates the effect of work hardening and causes new particles to start the densification process. This issue leads to the placement of a larger volume of particles in the grain boundaries, and the relative porosity of the samples decreases after ECAP (Ashwath and Xavior, 2014).

3.2.2. X-Ray Pattern of Bulk Samples

XRD patterns of bulk pure Al samples created by applying the ECAP process on the powders milled at various times of 6 to 24 hours are represented in Figure 14. As shown, increasing the initial milling time has a significant increase in the intensity of the peaks appeared in the bulk samples. The appearance of a new peak related to the (221) plane indicates the effect of the applied strain due to severe plastic deformation compared to the initial powder samples.

The X-ray diffraction patterns of the bulk composite obtained from applying ECAP on Al-ZrB_2 powder are shown in Figure 15. The intensity of the peaks has reached its maximum value for samples that have been mechanically alloyed for up to 12 hours, and then their intensity has decreased, but the width of the peaks has increased. After 18 hours, the trend of reducing the size of the crystallites stopped, and with additional milling, no noticeable changes could be seen in their size. The time of 12 hours of milling is considered the turning point and the time after which the rate of particle size reduction slows down and reaches a stable state. The increase in grain boundary energy, which results from very high applied strain, prevents the particles from fracture, and the grain boundaries act as places for the accumulation of dislocations. Dynamic recovery has occurred here, resulting in a decrease in particle energy, and as a result, particle refinement has been stopped (Montazeri-Pour et al., 2014).

The diffraction lines of ZrB_2 disappear due to the decrease in the size of ZrB_2 particles to the sub-micron size with the increase of mechanical alloying time. This issue is associated with the apparent change of the Al peak towards lower angles. Milling for more than 18 hours leads to the broadening of Al peaks and a decrease in their intensity, which indicates a reduction in the size of the crystallites and the accumulation of heterogeneous strain in the material (Zhang et al., 2016).

As mentioned, the appearance of new peaks in the samples consolidated by the ECAP method compared to the original powder samples (Figures 5 and 6) is definitely due to the high strain applied by the severe plastic deformation process, leading to the activation of new slip planes.

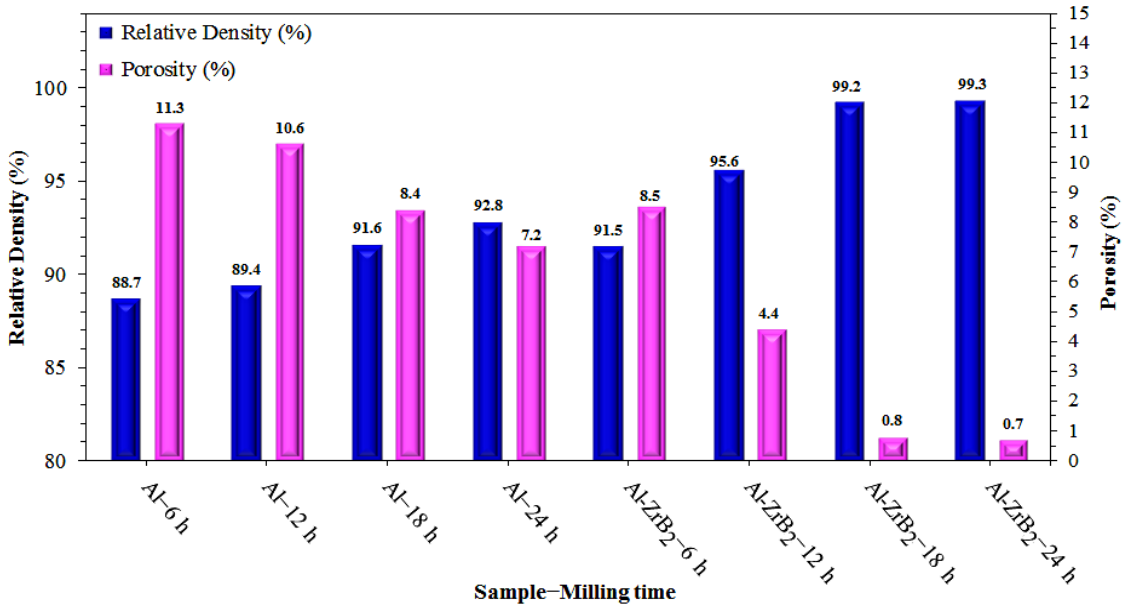

Figure 13. The density and the porosity of the bulk samples made by applying ECAP on the powders milled at 6, 12, 18, and 24 hours

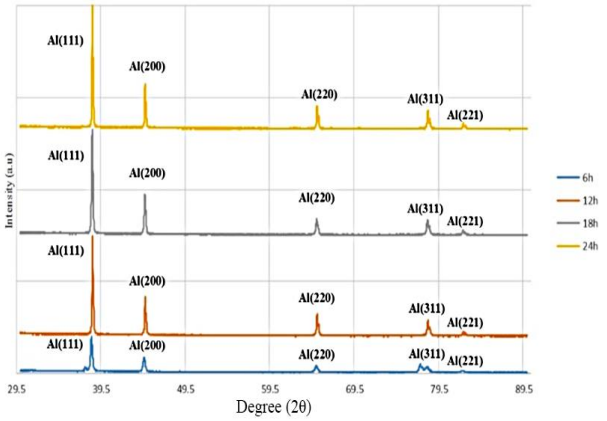

Figure 14. XRD diagrams of bulk pure aluminum samples fabricated by the applying ECAP process on powders resulting from milling for six up to 24 hours

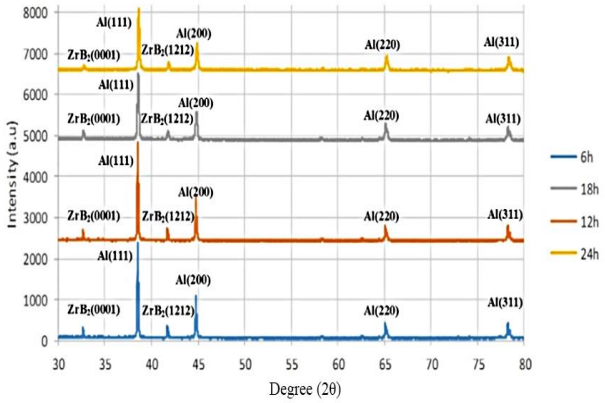

Figure 15. XRD of bulk Al-ZrB_2 samples produced by applying ECAP on powders resulting from mechanical alloying for six up to 24 hours

Figure 16 shows the changes in crystallite size and lattice strain for the bulk samples obtained by applying the ECAP process to pure Al and Al-ZrB_2 powders milled at varying times.

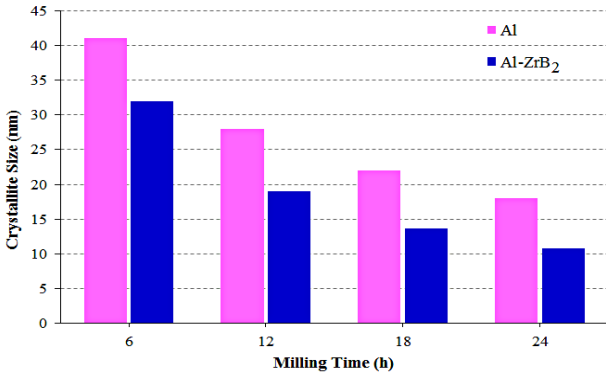

(a)

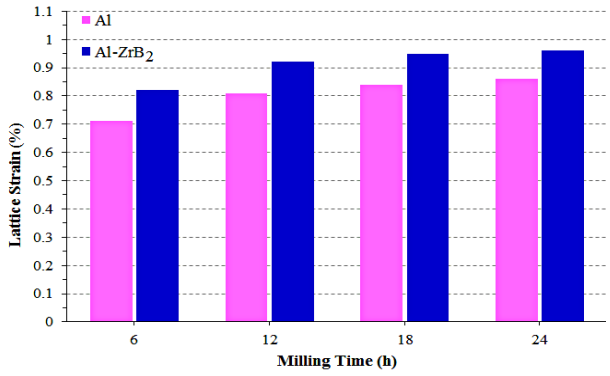

(b)

Figure 16. Column charts of (a) crystallite size and (b) lattice strain for the bulk pure Al and Al-ZrB_2 samples obtained from powders milled at various times of 6 hours up to 24 hours

As shown in Figure 16, the size of the crystallites of Al-5wt.% ZrB_2 MMC is finer than that of Al. In addition, the Al-ZrB_2 MMC sample obtained a higher lattice strain than the pure aluminum sample, and 12 hours of milling could be chosen as the turning point of the crystallite size reduction curve. The rate of crystallite size reduction decreased after 12 hours and remained almost constant after 18 hours. Hence, 18 hours could be selected as the optimum time for milling.

3.2.3. Microstructure of Bulk Samples

The microstructure obtained by optical microscopy for the Al and Al-ZrB_2 samples consolidated by ECAP is given in Figures 17 and 18, respectively. Visible holes in the obtained microstructure (Figure 17) result from burning impurities and electro-etching of the surface of the samples. All microstructures have fine precipitates in the matrix, which are finely dispersed throughout the grain boundaries in the structure of Al, and thus, homogeneity of composites increases (Asadipanah and Rajabi, 2015; Mohanavel et al., 2020). Herein, ZrB_2 particles appeared as spherical, angular, sub-angular, and scaly forms and distributed without forming agglomerates into the Al matrix (Alem et al., 2020b). Micrographs of an Al sample consolidated by the ECAP method with random morphology are shown in Figure 17 (a) up to (d). Al phase precipitates within and outside of grains make up the Al matrix, indicated with a white color (Alem et al., 2020a). A homogeneous dispersion of ZrB_2 particles significantly inhibits the development and expansion of large grains, as shown in Figure 18 (a) up to (d). Smaller particles have a stronger fixing impact on boundaries than larger particles. Dendritic structures indicate that ZrB_2 particulates are evenly distributed and the porosity is low, which motivates the development of a structure with more ZrB_2 in the Al matrix. Figure 18(d) shows that the dendrites are greatly enlarged.

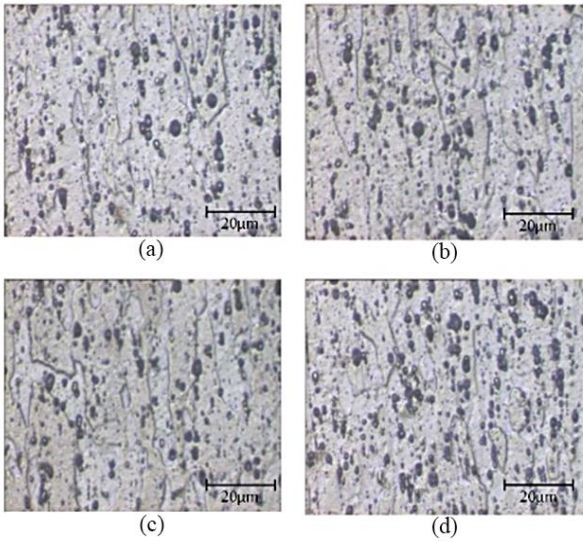

Figure 17. The optical microscopy images for the ECAP processed samples of pure Al produced by using powders milled for (a) 6 hours, (b) 12 hours, (c) 18 hours, and (d) 24 hours

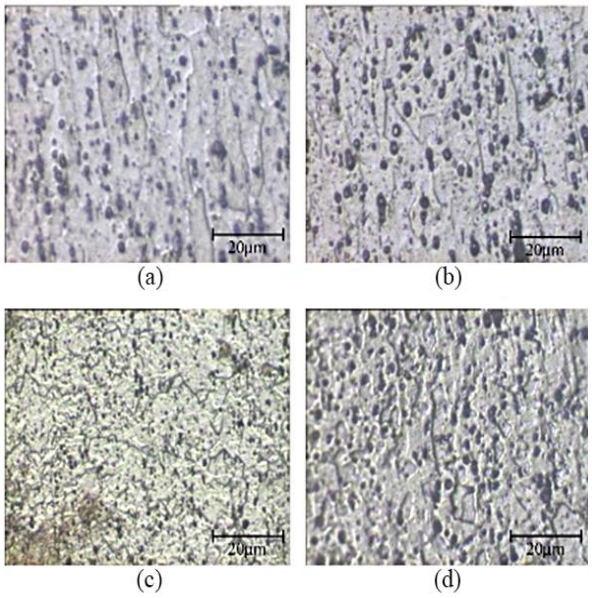

Figure 18. The optical microscopy images obtained for bulk samples of Al-ZrB_2 produced by using powders resulting from mechanical alloying for (a) 6 hours, (b) 12 hours, (c) 18 hours, and (d) 24 hours

The submicron structure obtained for the composite material is much more homogeneous than pure Al. The presence of hard ceramic particles and the accumulation of dislocations in the sub-grain and grain boundaries are the main motives for the UFG formation after the ECAP process. The obtained SEM images for bulk samples of Al-ZrB_2 milled at 6, 12, 18, and 24 hours are given in Figure 19. As can be seen, most grains contained small amounts of the secondary phase. Few grains contain cellular microstructures from the secondary phase, and their formation may have resulted from the secondary phase's sedimentation and agglomeration in the dendritic structure.

The difference in grain size from the surface to the center was due to the dynamic recovery phenomenon activated at this stage. As shown in Figure 19 (b), increasing the milling time by up to 12 hours has led to the diffusion of ZrB_2 particles in the grain boundaries. As shown in Figure 19 (d), increasing the mechanical alloying time up to 24 hours has led to larger grain sizes due to dynamic recovery as the dominant mechanism at this stage. The particles might not have had time to dissolve, so they diffused more at the grain boundaries. The increase in milling time and the crushing of aluminum particles decrease the amount of ZrB_2 in the grain boundaries, which is the reason for the dominance of the solid dissolution process in the more extended times of mechanical alloying. In addition, increasing the milling time leads to an increase in temperature, which increases the possibility of oxidation of aluminum. Finally, the defects created during the mechanical alloying time of 24 hours can be observed in Figure 19 (d).

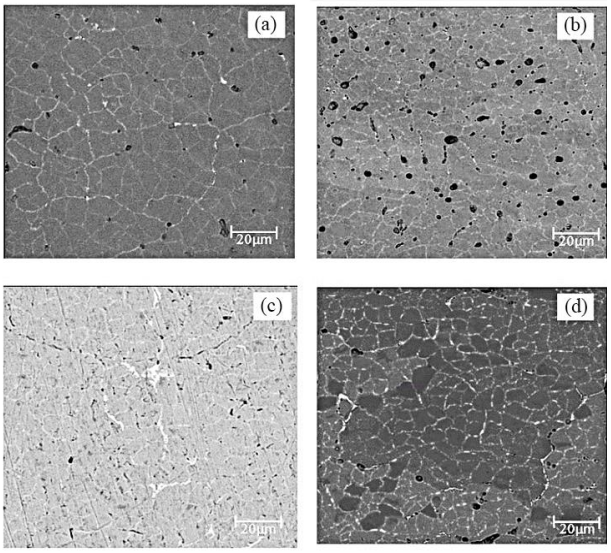

Figure 19. SEM images for ECAP processed bulk samples of Al-ZrB_2 produced by using powders resulting from mechanical alloying for (a) 6 hours, (b) 12 hours, (c)18 hours, and (d) 24 hours

As shown, the desired homogeneous microstructure corresponds to the milling time of 18 hours (Figure 19 (c)), indicating that the grains have completely refined at this stage. Therefore, the desired microstructure and, consequently, the desired mechanical properties are expected to be related to this case of mechanical alloying.

3.2.4. Micro-hardness of Bulk Samples

The effect of mechanical alloying time on the hardness properties of the bulk samples was evaluated using a micro-hardness tester. The results can be

observed in Figure 20, showing that the resulting micro-hardness increases at a high rate with the rise of mechanical alloying time up to 12 hours, but after this time, its rate is reduced until 24 hours when the trend of its increasing rate reaches its lowest level. Two active mechanisms could explain the increase in hardness of pure Al samples and Al-ZrB_2 MMC samples. One reason is the change in grain size and, consequently, the rise in grain boundaries, which in turn increases the hardness. The other mechanism is the increase in the density of dislocations due to the plastic deformation of particles during mechanical alloying and ECAP processes, which is known as the work hardening phenomenon. Aside from the two active mechanisms for both pure Al and Al-ZrB_2 MMC, there is also increased microhardness gradients for the Al-ZrB_2 MMC sample due to the high hardness of ZrB_2 particles and the hardening resulting from the dissolution of the secondary solid phase, compared to pure Al.

The dynamic recovery mechanism in the samples is expected to affect the trend of the grain size decrement during a further increase in milling time. Consequently, the rate of hardness increase would be reduced. Hence, the upward trend of increasing hardness continues until 24 hours of milling, but its increasing rate decreases after 12 hours of milling.

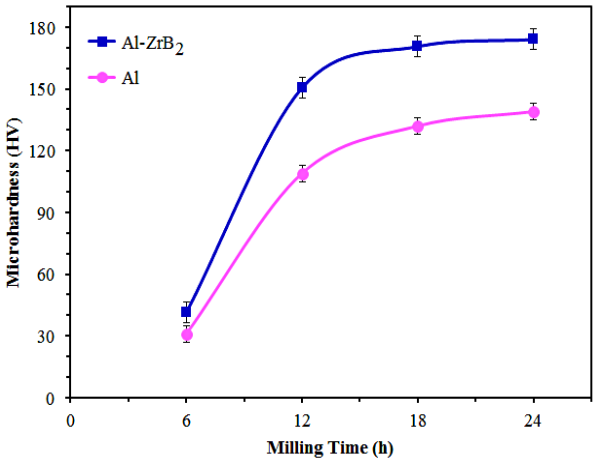

Figure 20. Micro-hardness (HV) changes for bulk pure Al and Al-ZrB_2 samples produced using powders milled for 6-24 hours

3.2.5. The Shear Punch Test of Bulk Samples

As summarized in column chart of Figure 21, the results of the shear punch test for ECAP-processed bulk Al-ZrB_2 samples indicate that the samples that have been mechanically alloyed for up to 24 hours have the highest strength due to having the minimum crystallite size.

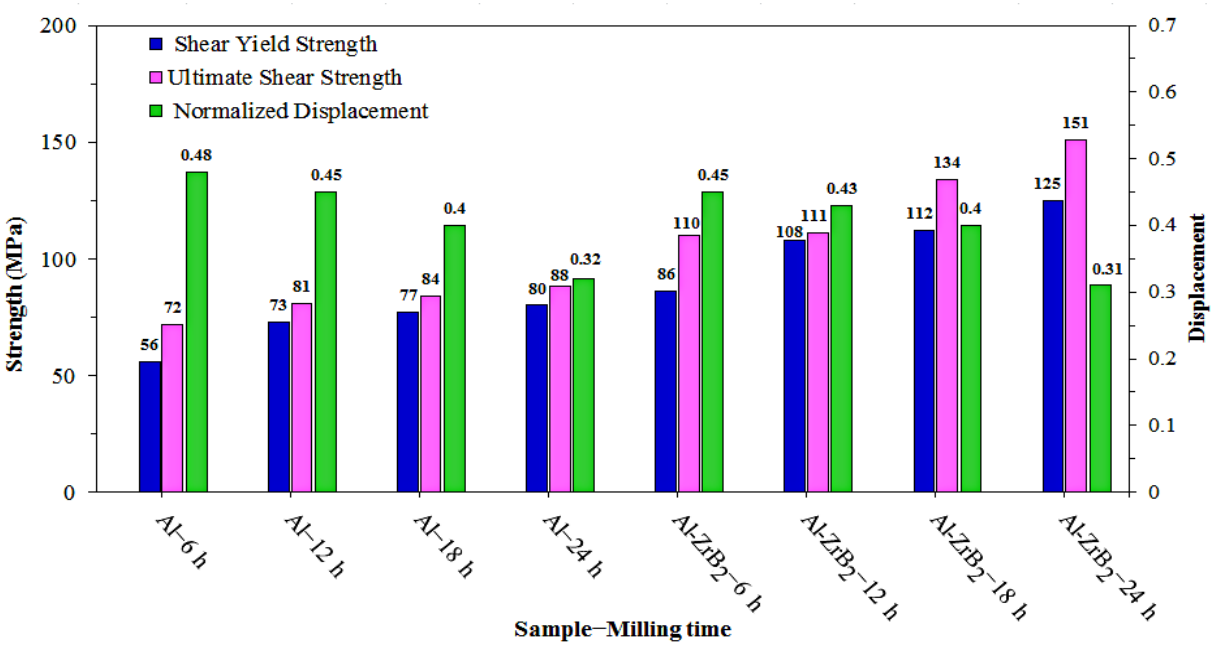

Figure 21. The shear punch test results of bulk samples produced by applying ECAP on pure aluminum and Al-ZrB_2 powders milled at different times

Conducting ECAP to compact samples causes the strength of the samples to be increased by a higher rate up to 12 hours of milling, and their strength changes slightly after that, up to 24 hours. The highest ductility is related to ECAP-processed samples produced using 6 hours of milling of pure Al and Al-ZrB_2 MMC powders, and the lowest ductility is related to bulk samples prepared using 24 hours of mechanical milling of both samples. This subject might be caused by the application of very high strain by the warm ECAP process (Iwahashi et al., 1996; Montazeri-Pour et al., 2014) and the work hardening phenomenon due to the deformation of

powders during the milling procedure (Suryanarayana et al., 2001).

In general, the absorption of dislocations by grain boundaries and the balance between work-hardening caused by severe plastic deformation and dynamic recovery have led to a decrease in the rate of grain size reduction (Montazeri-Pour and Parsa, 2016; Montazeri-Pour et al., 2014). Based on the calculated grain size, the rate of grain size reduction with increasing milling time was higher for Al-ZrB_2 MMC. The increase in the density of dislocations and their presence in the grain boundaries and the precipitation hardening resulting from Al-ZrB_2 MMC at higher times could lead to equilibrium or dynamic recovery. This issue is consistent with the lower grain size and the higher rate of grain size reduction of Al-ZrB_2 MMC compared to pure Al. The finer size of the crystallites and the increase of the lattice strain imply the grain size reduction with the increase of the milling time. The dominance of dynamic recovery over the hardening caused by the decrease in grain size can lead to the reduction of grain fracture rate. A dynamic recrystallization process and a relative increase in grain size are possible after 24 hours of milling. The border between the particles is the energy-rich area and the best area for the agglomeration of particles and the accumulation of impurities. The decrease in the density of holes in the boundary between grains shows that the energy of grain boundaries might be decreased during 24 hours of milling. In other words, a decrease in grain boundaries can have been happening, which confirms dynamic recovery at times longer than 18 hours of mechanical alloying (Alem et al., 2020b; Yadav Kaku et al., 2018).

4. CONCLUSIONS

Applying the warm ECAP process at 250°C on the Al-ZrB_2 composite powder obtained by milling for up to 24 hours improved the mechanical and physical properties of the obtained samples. The achieved microstructure became more homogeneous with the increase of the milling time. In addition, producing samples using the ECAP method significantly affected the homogeneity of the microstructure and the refinement of the grains. The milling time of 12 hours is introduced as the turning point of the mechanical alloying time. After that, the mechanical properties increased slowly, the grain size reduction rate decreased, and consequently, the microstructure homogenization rate decreased. Performing severe plastic deformation by the ECAP method on powder samples, turning them into bulk samples with this method, and increasing the mechanical alloying time improved the mechanical properties of Al-5wt% ZrB_2 MMC samples. However, its rate decreased after 12 hours of mechanical alloying, and finally, it reached a stable state after 18 hours, and no significant changes were observed in mechanical properties up to 24 hours. The results of the shear punch test of Al-5 wt.% ZrB_2 MMC samples indicated that the samples that have been mechanically alloyed for up to 24 hours had the highest strength. Therefore, the production of Al-ZrB_2 MMC by powder metallurgy method found a favorable result through the ECAP process for the consolidation of powders milled for 24 hours.

ACKNOWLEDGEMENT

The authors gratefully acknowledge Imam Khomeini International University (IKIU) for providing the financial support of this work.

Declaration of Competing Interest

The authors declared no conflicts of interest.

REFERENCES

1. Alem, S. A. A., Latifi, R., Angizi, S., Hassanaghaei, F., Aghaahmadi, M., Ghasali, E., & Rajabi, M. (2020a). Microwave sintering of ceramic reinforced metal matrix composites and their properties: a review. *Materials and Manufacturing Processes*, Vol. *35*(3), 303-327. https://doi.org/10.1080/10426914.2020.1718698
2. Alem, S. A. A., Latifi, R., Angizi, S., Mohamadbeigi, N., Rajabi, M., Ghasali, E., & Orooji, Y. (2020b). Development of metal matrix composites and nanocomposites via double-pressing double-sintering (DPDS) method. *Materials Today Communications*, Vol. *25*, 101245. https://doi.org/10.1016/j.mtcomm.2020.101245
3. Asadipanah, Z., & Rajabi, M. (2015). Production of Al–ZrB_2 nano-composites by microwave sintering process. *Journal of Materials Science: Materials in Electronics*, Vol. *26*(8), 6148-6156. https://doi.org/10.1007/s10854-015-3195-9
4. Ashwath, P., & Xavior, M. A. (2014). The effect of ball milling & reinforcement percentage on sintered samples of aluminium alloy metal matrix composites. *Procedia Engineering*, Vol. *97*, 1027-1032. https://doi.org/10.1016/j.proeng.2014.12.380
5. ASTM B311-22. (2022). Standard Test Method for Density of Powder Metallurgy (PM) Materials Containing Less Than Two Percent Porosity. In: ASTM International. https://www.astm.org/b0311-17.html
6. Bhat, A., Budholiya, S., Raj, S. A., Sultan, M. T. H., Hui, D., Shah, A. U. M., & Safri, S. N. A. (2021). Review on nanocomposites based on aerospace applications. *Nanotechnology Reviews*, Vol. *10*(1), 237-253. https://doi.org/10.1515/ntrev-2021-0018
7. Bhoi, N. K., Singh, H., & Pratap, S. (2019). Developments in the aluminum metal matrix composites reinforced by micro/nano particles – A review. *Journal of Composite Materials*, Vol. *54*(6), 813-833. https://doi.org/10.1177/0021998319865307
8. Brodova, I. G., Petrova, A. N., Shirinkina, I. G., Rasposienko, D. Y., Yolshina, L. A., Muradymov, R. V.,…Shorokhov, E. V. (2021). Mechanical properties of submicrocrystalline aluminium matrix composites reinforced by in situ graphene through severe plastic deformation processes. *Journal of Alloys and Compounds*, Vol. *859*, 158387. https://doi.org/10.1016/j.jallcom.2020.158387
9. Chak, V., Chattopadhyay, H., & Dora, T. L. (2020). A review on fabrication methods, reinforcements and mechanical properties of aluminum matrix composites. *Journal of Manufacturing Processes*, Vol. *56*, 1059-1074. https://doi.org/10.1016/j.jmapro.2020.05.042
10. Chandel, R., Sharma, N., & Bansal, S. A. (2021). A review on recent developments of aluminum-based hybrid composites for automotive applications. *Emergent Materials*, Vol. *4*(5), 1243-1257. https://doi.org/10.1007/s42247-021-00186-6

11. Diler, E. A., & Ipek, R. (2012). An experimental and statistical study of interaction effects of matrix particle size, reinforcement particle size and volume fraction on the flexural strength of Al–SiCp composites by P/M using central composite design. *Materials Science and Engineering: A*, Vol. *548*, 43-55. https://doi.org/10.1016/j.msea.2012.03.066
12. Ebrahimi, M., & Wang, Q. (2022). Accumulative roll-bonding of aluminum alloys and composites: An overview of properties and performance. *Journal of Materials Research and Technology*, Vol. *19*, 4381-4403. https://doi.org/10.1016/j.jmrt.2022.06.175
13. Edalati, K., & Horita, Z. (2016). A review on high-pressure torsion (HPT) from 1935 to 1988. *Materials Science and Engineering: A*, Vol. *652*, 325-352. https://doi.org/10.1016/j.msea.2015.11.074
14. Erturun, V., Çetin, S., & Sahin, O. (2021). Investigation of microstructure of aluminum based composite material obtained by mechanical alloying. *Metals and Materials International*, Vol. *27*(6), 1662-1670. https://doi.org/10.1007/s12540-019-00583-x
15. Faraji, G., Kim, H. S., & Kashi, H. T. (2018). Chapter 2 - Severe Plastic Deformation Methods for Bulk Samples. In G. Faraji, H. S. Kim, & H. T. Kashi (Eds.), *Severe Plastic Deformation* (pp. 37-112). Elsevier. https://doi.org/10.1016/B978-0-12-813518-1.00002-3
16. Gajević, S., Miladinović, S., & Stojanović, B. (2022). Chapter 8 - Metallic nanocomposites: An Introduction. In H. Song, T. A. Nguyen, G. Yasin, N. B. Singh, & R. K. Gupta (Eds.), *Nanotechnology in the Automotive Industry* (pp. 155-161). Elsevier. https://doi.org/10.1016/B978-0-323-90524-4.00008-6
17. Gao, Q., Deane, G. B., & Shen, L. (2021). Bubble production by air filament and cavity breakup in plunging breaking wave crests. *Journal of Fluid Mechanics*, Vol. *929*, A44, Article A44. https://doi.org/10.1017/jfm.2021.890
18. Hamilton, J. D., Ramesh, S., Harrysson, O. L., Rock, C. D., & Rivero, I. V. (2021). Cryogenic mechanical alloying of aluminum matrix composites for powder bed fusion additive manufacturing. *Journal of Composite Materials*, Vol. *55*(5), 641-651. https://doi.org/10.1177/0021998320957698
19. Iwahashi, Y., Wang, J., Horita, Z., Nemoto, M., & Langdon, T. G. (1996). Principle of equal-channel angular peessing for the processing of ultra-fine grained materials. *Scripta Materialia*, Vol. *35*, 143–146. https://doi.org/10.1016/1359-6462(96)00107-8
20. Kumar, B., & Kumar, P. (2022). Preparation of hybrid reinforced aluminium metal matrix composite by using ZrB_2: A systematic review. *Materials Today: Proceedings*, Vol. *61*, 115-120. https://doi.org/10.1016/j.matpr.2022.04.066
21. Kumar, S. D., Ravichandran, M., Jeevika, A., Stalin, B., Kailasanathan, C., & Karthick, A. (2021). Effect of ZrB_2 on microstructural, mechanical and corrosion behaviour of aluminium (AA7178) alloy matrix composite prepared by the stir casting route. *Ceramics International*, Vol. *47*(9), 12951-12962. https://doi.org/10.1016/j.ceramint.2021.01.158
22. Lakshmikanthan, A., Angadi, S., Malik, V., Saxena, K. K., Prakash, C., Dixit, S., & Mohammed, K. A. (2022). Mechanical and tribological properties of aluminum-based metal-matrix composites. *Materials*, Vol. *15*(17), 6111. https://doi.org/10.3390/ma15176111
23. Maurice, D., & Courtney, T. H. (1994). Modeling of mechanical alloying: Part I. deformation, coalescence, bdand fragmentation mechanisms. *Metallurgical and Materials Transactions A*, Vol. *25*(1), 147-158. https://doi.org/10.1007/BF02646683
24. Mohanavel, V., Ravichandran, M., & Suresh Kumar, S. (2020). Tribological and mechanical properties of Zirconium Di-boride (ZrB_2) particles reinforced aluminium matrix composites. *Materials Today: Proceedings*, Vol. *21*, 862-864. https://doi.org/10.1016/j.matpr.2019.07.603
25. Montazeri-Pour, M., & Parsa, M. H. (2016). Constitutive analysis of tensile deformation behavior for AA1100 aluminum subjected to multi-axial incremental forging and shearing. *Mechanics of Materials*, Vol. *94*, 117-131. https://doi.org/10.1016/j.mechmat.2015.11.016
26. Montazeri-Pour, M., Parsa, M. H., Jafarian, H. R., & Taieban, S. (2015a). Microstructural and mechanical properties of AA1100 aluminum processed by multi-axial incremental forging and shearing. *Materials Science and Engineering A*, Vol. *639*, 705–716. https://doi.org/10.1016/j.msea.2015.05.066
27. Montazeri-Pour, M., Parsa, M. H., Khajezade, A., & Mirzadeh, H. (2015b). Multi-axial incremental forging and shearing as a new severe plastic deformation processing technique. *Advanced Engineering Materials*, Vol. *17*(8), 1197-1207. https://doi.org/10.1002/adem.201400467
28. Montazeri-Pour, M., Parsa, M. H., & Mirzadeh, H. (2014). Constitutive description of severely deformed metals based on dimensional analysis. *Materials Science and Technology*, Vol. *30*(6), 719-724. https://doi.org/10.1179/1743284713y.0000000424
29. Patra, A., Karak, S. K., & Pal, S. (2016). Effects of mechanical alloying on solid solubility. *Advanced Engineering Forum*, Vol. *15*, 17–24. https://doi.org/10.4028/www.scientific.net/aef.15.17
30. Sharma, S. K., Saxena, K. K., Salem, K. H., Mohammed, K. A., Singh, R., & Prakash, C. (2024). Effects of various fabrication techniques on the mechanical characteristics of metal matrix composites: a review. *Advances in Materials and Processing Technologies*, Vol. *10*(2), 277-294. https://doi.org/10.1080/2374068X.2022.2144276
31. Suryanarayana, C. (1999). Chapter 4- Mechanical alloying. In C. Suryanarayana (Ed.), *Pergamon Materials Series* (Vol. 2, pp. 49-85). Pergamon. https://doi.org/10.1016/S1470-1804(99)80050-9
32. Suryanarayana, C., Ivanov, E., & Boldyrev, V. V. (2001). The science and technology of mechanical alloying. *Materials Science and Engineering: A*, Vol. *304-306*, 151-158. https://doi.org/10.1016/S0921-5093(00)01465-9
33. Vishnu, P., Raj Mohan, R., Krishna Sangeethaa, E., Raghuraman, S., & Venkatraman, R. (2020). A review on processing of aluminium and its alloys through Equal Channel Angular Pressing die. *Materials Today: Proceedings*, Vol. *21*, 212-222. https://doi.org/10.1016/j.matpr.2019.04.223
34. Yadav Kaku, S. M., Raju, V., Bharath, K., Fuchs Godec, R., & Reddy Tiyyagura, H. (2018). Evaluation of ZrB_2 reinforced Al/Al alloy composite produced by powder metallurgy-vacuum arc melting technique: A unique approach. *Vacuum*, Vol. *155*, 539-545. https://doi.org/10.1016/j.vacuum.2018.06.055
35. Yue, H., Yao, L., Gao, X., Zhang, S., Guo, E., Zhang, H.,…Wang, B. (2017). Effect of ball-milling and graphene contents on the mechanical properties and fracture mechanisms of graphene nanosheets reinforced copper matrix composites. *Journal of Alloys and Compounds*, Vol. *691*, 755-762. https://doi.org/10.1016/j.jallcom.2016.08.303
36. Zhang, H., Xu, C., Xiao, W., Ameyama, K., & Ma, C. (2016). Enhanced mechanical properties of Al5083 alloy with graphene nanoplates prepared by ball milling and hot extrusion. *Materials Science and Engineering: A*, Vol. *658*, 8-15. https://doi.org/10.1016/j.msea.2016.01.076